SLOPE, ELEVATION, AND THERMAL INERTIA TRENDS OF RECURRING SLOPE LINEAE: RSL INITIATION AND TERMINATION POINTS FALL OUTSIDE THE ANGLE OF REPOSE.

Michelle Tebolt[1], Norbert Schorghofer[2], Timothy Goudge[3], & Joseph Levy[1] [1]Colgate University, 13 Oak Ave., Hamilton, NY, mtebolt@colgate.edu, [2]Planetary Science Institute, Tucson AZ, [3]University of Texas at Austin, Austin, TX.

Background: Recurring slope lineae (RSL) are dark linear features that occur on the surface of steep slopes in the mid-latitudes of Mars. These areas are warm, occasionally exceeding temperatures of 273-320 K [1-2]. RSL recur over multiple years, growing during warm seasons and fading away during colder seasons [3]. Their apparent temperature dependency raises the possibility that liquid water is involved in their formation. Possible "wet" formation processes include melting shallow ice or ground water [3], or deliquescence of soil salts, as CRISM data has shown hydrated salts present at some RSL sites [4], although band identifications have recently been challenged [5]. Possible "dry" formation processes include mass wasting [3], dry granular flow triggered by an aeolian recirculating system [6], or sublimation of frozen CO_2 trapped in the soil [7].

Here, we consider how the physical characteristics of the RSL can be used to evaluate these competing hypotheses. The elevation, slope, and thermal inertia characteristics of RSL should differ depending on whether the features are caused by wet or dry flow. If RSL are caused by mass wasting or granular flow, the features should end at slopes between 28˚ and 35˚, the angle of repose for fine martian sediment [6]. If RSL are caused by gas-triggered granular flow, the features would be expected to start on slopes between 23˚ and 36˚, where the terrain will be steep enough to cause the dry, initially-settled grains to tumble downslope [7]. Finally, thermal inertia is associated with surficial sediment grain size [15], allowing RSL sites to be sedimentologically characterized.

Methods: HiRISE images with a resolution of 25 cm/px were used to map a total of 12,736 RSL across 17 different confirmed RSL sites across the mid-latitudes of Mars [1,3,8]. The upslope and downslope terminal points (tops and bottoms) of each RSL were mapped during the time of maximum RSL extent. RSL are typically dendritic, leading to multiple top points being coded to a single RSL bottom point where dark lineations meet. Elevation and slope were determined using the stereo DEM of each site, which was constructed from linked HiRISE and CTX stereo pairs using the open source NASA Ames Stereo Pipeline (ASP) [9-13]. The slope of each point was found by taking the average slope within a 1 m buffer around the tops and bottoms of the features. To calculate the length of each RSL, the distance between each beginning and end point was calculated in three dimensions and averaged together to get a single length for each individual RSL.

THEMIS derived global thermal inertia data [14], with a resolution of 100 m/px, were sampled at top and bottom points. Elevation, slope, and thermal inertia were also extracted at 10,000 randomly selected points located across the HiRISE image and within the RSL hillslope (a convex hull containing all mapped RSL). Together, these measurements determine if slopes of the tops and bottoms fall within the predicted angles of repose for dry flows.

Results: RSL typically occur at the highest elevation values of each site. This is common across most of the 17 sites, but the absolute elevation of the RSL varies depending on the elevation of the site as a whole. The thermal inertia of the RSL are higher than the typical thermal inertia values across the mapping site by about 200 TIU (Fig. 1). RSL typically form on surfaces with 300 to 800 TIU (Fig. 1).

The RSL initiate on slopes that tend to be steeper than the average slopes across the entire site. As expected, the tops are steeper than bottoms with a typical difference of ~4˚-10˚ (Fig. 2).

The angle of repose for gas-triggered granular flow is estimated to be between 23˚ and 36˚ for the tops of the RSL [7]. In this study, 54% of the RSL tops begin at slopes greater than 36˚, 42% begin at slopes between 23˚- 36˚, and the remaining 4% begin at slopes below 23˚.

The angle of repose for the termination points of granular flow is estimated to be between 28˚ and 35˚ [6]. We found that 26% of the RSL bottoms occur at slopes exceeding 35˚, 49% fall between 28˚- 35˚, and 25% end on slopes shallower than 28˚.

One notable observation of the RSL morphology emerging from this investigation is detection of occasional discontinuous RSL darkening features. These were particularly evident in Palikir Crater (Fig. 3), with dark patches of RSL appearing further downslope of the majority of the RSL population. The discontinuities were then included in the RSL network over time as the main features grew and extended to these lower elevations.

Discussion: The elevation trends of RSL are relevant when considering potential formation

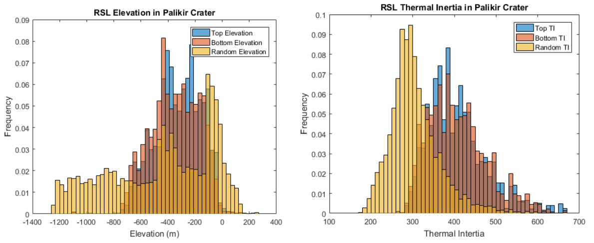

Fig. 1. Elevation and thermal inertia trends of RSL and randomly selected background points across the representative site of Palikir Crater.

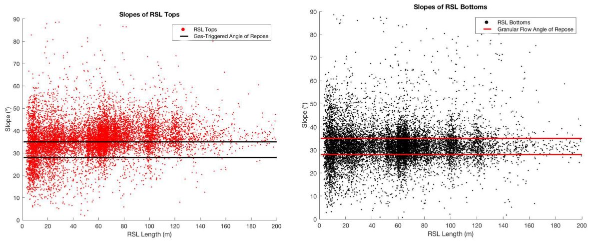

Fig. 2. Slopes of RSL tops and bottoms plotted against length with relation to the angles of repose [6,7]. 98% of the RSL have a length ≤ 200m. The figure only includes these RSL for clarity.

mechanisms for the features. Unconfined groundwater discharges at the surface at low elevations where the water table first intersects surface topography. The opposite behavior occurs here, with the RSL forming on the highest, steepest elevations at each site. Confined aquifers may discharge higher where aquicludes or pressurized fluids intersect the surface; however, RSL commonly emerge near topographic divides (e.g., bedrock knobs or crater rims), limiting subsurface connectivity. RSL may be confined to higher elevations due to the lack of shadows, and direct exposure to sun, resulting in intense warming.

RSL also have distinguishing thermal inertia trends. The RSL thermal inertia values are consistent with sand, as sand-sized particles typically have a thermal inertia around 400 TIU [14]. It has been widely noted that RSL first become visible on slopes beneath bedrock outcrops. This means that the RSL first appear at bedrock-sand interfaces, and are only observed to advance on sediment-covered slopes—never crossing bedrock. One possibility is that sand may be necessary to distinguish the features from their surroundings due to greater albedo change from wetting or roughness changes for sediments vs. bedrock [16].

The slopes of the RSL are also notable. If the features are caused by gas-triggered granular flow, it would be unusual for the majority of them to start at slopes greater than 36°. These slopes are steep enough that sediment should immediately begin downslope flow without any gas-trigger, yet about 54% of the RSL begin at such steep slopes (suggesting a possible role for grain cohesion or cementation). It may be that the RSL actually begin further upslope, but only become visible in these sandy areas. Additionally, about 440 of the RSL begin at slopes less than 23°, which is too shallow to initiate dry sediment gravity flows. About a quarter of all RSL stop at slopes shallower than the angle of repose. These slope trends indicate that granular flow is unlikely to be the only mechanism forming RSL. Somehow, RSL must be able to propagate across slopes that are too shallow to initiate or sustain dry or gas-triggered mass movement of sandy sediment.

The observation of discontinuous features also challenges the granular flow model of RSL. If the RSL are caused by granular flow, the sediment should travel downslope in a continuous path, maintaining a connection to its source. Instead, dark, discontinuous, patches appear downslope of the RSL and only connect later in the season (Figure 3). These features could be explained if the RSL are caused by shallow groundwater, as the water could differentially reach the surface as a function of ice table depth, capillary rise, or discharge routing [17-18].

References: [1] Ojha. L, et al. (2014) *Icar, 231*, 365–76. [2] Schorghofer, N., et al. (2018) *AGU FM,* P53F-3024. [3] McEwen, A S., et al. (2014) *Nat. Geo., 7*, 53–58. [4] Ojha, L., et al. (2015) *Nat. Geo., 8*, 829–32. [5] Vincendon, M., et al. (2018) arXiv:1808.09699. [6] Dundas, C.M., et al. (2017) *Nat. Geo., 10*, 903–7. [7] Schmidt, F., et al. (2017) *Nat. Geo, 10*, 270–73. [8] Stillman, D E., et al. (2016) *Icarus, 265*, 125–38. [9] Broxton M.J. & Edwards L.J., (2008) *39th LPSC* Abstr. #2419. [10] Moratto, et al. (2010) *41st LPSC*, Abstr. 1533. [11] Beyer, R.A., et al. (2014). *45th LPSC,* Abstr. 2902. [12] Beyer, R.A., et al. (2018) *E&SS*, *5*, 537–48. [13] Shean, et al. (2016) *ISPRS J. Photogram & Remote Sensing, 116*, 101-117. [14] Fergason, R. L., et al. (2006) *JGR*, *111*, E12. [15] Golombek M.P., et al., (2001) *1st MER Land. Site Workshop,* 27-28. [16] Twomey, S.A., et al. (1986) *Ap. Optics*, *25*, 431-437. [17] Gooseff M.N., et al. (2013) *Hydro. J., 21*, 171–183. [18] Levy, J. et al. (2014) *Ant. Sci.*, *26*, 565–72.

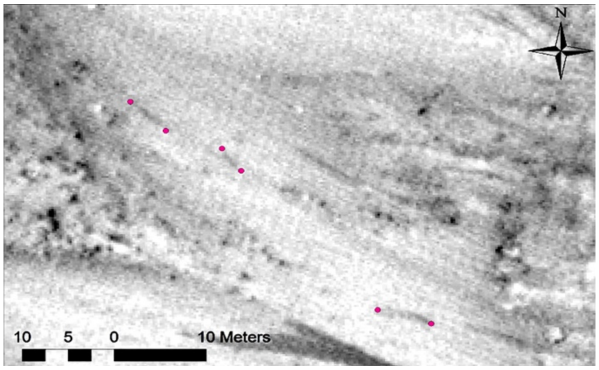

Fig. 3. Discontinuous RSL at Palikir Crater. RSL segments sharing a similar downslope pathway that become linked later in the year are marked with pink dots. Portion of HiRISE image ESP_022689_1380.